

# Chapter 7

## Feasibility Analysis of Solar Tracking Technologies Connected to Renewable Energy Systems



Reza Babaei, David S.-K. Ting, and Rupp Carriveau

**Abstract** The environmental benefits of photovoltaic (PV) panels have attracted attention worldwide although they still lack the necessary levels of performance and financial viability. To meet these standards, PV tracking technologies are utilized to maximize the efficiency of PV systems. The principal goal of this research work is to perform a techno-economic feasibility analysis and optimal sizing of renewable energy systems integrated into solar tracking technologies for a rural residential user in South Africa. The vertical axis (VC), dual-axis tracker (DA), horizontal axis with monthly (HM), and continuous (HC) adjustments are the tracking options implemented to determine a profitable energy system. The preferred optimal cases based on these scenarios are introduced, and then sensitivity analysis is carried out to estimate the effect of variation of technical, economic, and climatic parameters. The VC-based system offers a financially desirable alternative having net present cost (NPC), levelized energy cost (LCOE), and CO<sub>2</sub> emissions of \$13.7k, \$0.258/kWh, and 2.81.1 kg/year, respectively. Sensitivity analysis indicates that an increase in SOC<sub>min</sub> would raise NPC and CO<sub>2</sub> emissions. The DA and VC trackers, respectively, show the greatest and lowest increases in NPC due to diesel prices increase. In VC and HM-based cases, PV generation and the renewable fraction are more sensitive to albedo (ground reflectance) variation. Comparing the current optimal results with the previous research in this location demonstrates that NPC and LCOE can be reduced by implementing a proper controlling strategy by \$58k and \$0.005/kWh, respectively, to meet the same electrical load.

**Keywords** PV tracker · Microgrids · Hybrid energy systems · Photovoltaics · Renewable energy

---

R. Babaei (✉) · D. S.-K. Ting · R. Carriveau  
Turbulence and Energy Laboratory, University of Windsor, 401 Sunset Ave, Windsor, ON, Canada  
e-mail: [babaeij@uwindsor.ca](mailto:babaeij@uwindsor.ca)

## Nomenclature

DA	Dual-axis tracker
DG	Diesel generator
$F_1$	Fuel curve slope (L/h/ output kW or m <sup>3</sup> /h/output kW)
$F_o$	Generator fuel curve intercept co-efficient (L/h/rated kW or m <sup>3</sup> /h/rated kW)
$f_{pv}$	PV derating factor (%)
FT	Fixed tilt
GS	Incident radiation at standard test conditions (1 kW/m <sup>2</sup> )
GT	Solar radiation incident in the current hour (kW/m <sup>2</sup> )
HKT	Hydrokinetic turbine
HM	Horizontal axis
HV	Vertical axis
LCOE	Levelized cost of energy(\$/kWh)
$L_{max}$	Absorption width in maximum power
NPC	Net present cost
O&M	Operation and maintenance cost
$P_{DG}$	Generator output power (kW)
$P_{DG}$	Rated generator power (kW)
$P_{max}$	Maximum available power
PV	Solar photovoltaic
Q	Energy available in the storage at the first timestep (kWh)
$Q_1$	Available energy remained at the first timestep (kWh)
$W_{pv}$	Peak power output of PV array (kW)
$Y_{DG}$	Rated capacity of the generator (kW)
$\eta_{DG}$	Generator efficiency (%)

## 7.1 Introduction

Access to electricity is a critical indicator which impacts the social and financial progress of regions [1]. In this regard, energy scarcity, power instability, and electricity outages have grown worldwide, notably in Africa, where high costs and erratically insufficient electricity have severely affected people's lives [2–4].

Among African countries, South Africa has a large number of rural and energy-deprived populations in which electricity is unavailable to around 30% of rural South Africans. To address this issue, renewable energy can be an environmentally friendly and economical approach to deal with outages and shortages of electricity [5]. Figure 7.1 demonstrates electricity access in rural areas in South Africa and (b) South Africa's electricity production by technology category. The electricity generated by coal as a crucial non-renewable source is predicted to decrease by 150 TWh by 2040. Electricity access has been inconsistent during the past decade in Africa although it started to gradually expand in 2016.

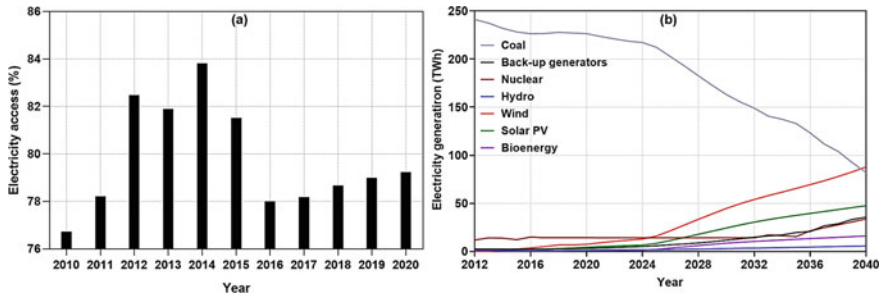


**Fig. 7.1** The presentation of **a** electricity access in rural localities and **b** electricity production by technology in South Africa

Solar, wind, geothermal, biomass, and nuclear energy are deemed to be the ideal renewable energy sources for electrification. Another preferable method to provide electricity is to utilize the potential of rivers and oceans, which is known as hydrokinetic (HKT) [6]. With hydrokinetic technology, energy can be converted in a way that has minimal negative effects on the environment. Such as technology has the potential to satisfy the electricity requirements of remote communities, particularly energy-deprived regions in South Africa [7]. The configuration for installing these types of turbines has been demonstrated to be safe and reliable, with minimal environmental impact on the environment. Having mentioned the unique features, there have been a few feasibility research articles on employing micro hydrokinetic power plants to deliver electricity to rural areas.

Despite the described preferred properties of the renewable energy components, the negative of this technology is that the power output varies from hour to hour, resulting in unreliability to supply the load during a day with consistent intensity [8]. Since renewable resources highly depend on meteorological data, and energy storage configuration which makes it challenging to maintain the energy at a certain level of intensity [9, 10].

Some of the previous research articles have investigated the techno-economic feasibility evaluation of these renewable hybrid energy systems (HES) in rural or remote areas. The general category of these studies can be divided into three main groups: optimization algorithm [11–13], design and planning [14–17], comparison procedure [18–20], and energy management [21–23]. For instance, Ref. [24] proposed PV/WT/HKT (Hydrokinetic turbine) system for grid-independent electrification. The findings revealed that this energy solution might be cost-effective and influential in remote regions where grid connectivity is either prohibitively costly or impossible. In Saint Catherine, Egypt, Ref. [25] employed a PV/WT/FC/DG/Hybrid natural gas turbine option to meet a household load of 80 kWh/d. The paper utilized a bi-directional ant colony algorithm to develop a strategy for building optimum systems while minimizing NPC and GHG emissions equally. Ref. [26] also provided an ideal and cost-effective hybrid energy source for a farming community and a suburban neighborhood in a small hamlet in Punjab, Pakistan, utilizing a PV/biomass

configuration. The best solution demonstrated energy and net present cost that were both techno-economically realistic, allowing them to be grid-independent. Reference [27] conducted a techno-economic feasibility analysis through PV/DG system for a small-scale load requirement. They stated that a \$2,300 salvage cost would result from initial costs of \$26,150 being invested. Reference [28] analyzed off-grid PV/WT/DG/biogas generator (BG), and grid-connected PV/WT designs are shown to be the best options. The grid-connected PV/WT was discovered to have a NPC of \$6.63M and an energy cost of \$0.0234/kWh. The NPC of the hybrid PV/WT/DG/BG is accounted for at \$18.1\$ and \$0.1251/kWh, respectively.

The PV system has shown significant improvement and stability in terms of energy generation among the studied renewable energy devices [29–31]. PV systems are becoming more popular owing to their low operating and maintenance costs (O&M) and convenience of usage in addressing rising power demands [8]. PV systems are extremely reliant on local irradiation variations; They are one of the fastest-growing alternatives because they transform solar irradiation into electricity [29]. In this respect, PV tracker techniques can be applied to absorb higher solar energy. Solar tracking system sets the PV collector in the ideal position for receiving the maximum energy [32]. The tracking mechanism can be used as per a single axis (single-axis tracker) or two axes (dual-axis tracker) with dual-axis tracking systems. However, there is an increase in investment and complications in using the two-axis tracking system [33]. In this respect, some previous articles have evaluated the technical, economic, and environmental aspects of tracking technologies integrated into HES. Table 7.1 summarizes the studies that have investigated the optimal sizing and feasibility analysis of PV tracking technology including vertical axis (VC), dual-axis tracker (DA), horizontal axis with monthly (HM), and continuous (HC) adjustments.

When considering the allocation of funds for solar energy systems, the choice between investing in a solar tracker or additional panels emerges as a critical decision with profound implications for overall system performance and financial viability. Several pivotal factors must be taken into account, including solar resource availability, electricity demand profile, and the prevailing costs of solar panels and trackers. Extensive research and studies have substantiated that solar trackers can significantly enhance energy generation, especially in regions with abundant solar irradiance and high energy demand during peak sunlight hours. The dynamic tracking ability of solar trackers optimizes energy capture, leading to a reduction in the number of panels required to achieve the desired energy output, thus not only lowering initial investment costs but also ensuring higher energy yields and better returns on investment [40].

Furthermore, the cost-effectiveness of solar trackers is particularly pronounced in off-grid and remote areas, where optimizing energy production and minimizing expenses are paramount considerations. The continuous adjustment of solar trackers to follow the sun's path ensures increased energy output, even in locations with variable weather conditions. Moreover, ongoing advancements in solar tracking technology and photovoltaic panel efficiencies bolster the case for the adoption of solar trackers as a compelling option. A comprehensive techno-economic analysis, encompassing factors such as the levelized cost of energy (LCOE), government incentives,

**Table 7.1** Summary of the previous research papers analyzing impacts of PV tracker devices

Grid connectivity	References	Year	Area	Energy system	Analyzed PV tracker
Off	[34]	2016	Hilly terrain, India	1. Photovoltaic 2. Wind turbine	1. HA 2. Fixed tilt 3. Azimuth tracking 4. DA
	[35]	2017	Eight areas in India	1. Photovoltaic	1. Fixed tilt 2. DA
	[36]	2016	Urumqi, China	1. Photovoltaic 2. Diesel generator	1. Fixed tilt 2. Single axis 3. DA
	[37]	2019	Rural healthcare building, India	1. Photovoltaic	1. HA 2. VA 2. DA
On	[38]	2017	Makkah, Saudi Arabia	1. Photovoltaic	1. HA 2. VA 3. DA
	[39]	2020	Alkharj City, Saudi Arabia	1. Photovoltaic 2. Fuel cell 3. Electrolyzer	1. HA 2. VA 3. DA

and available rebates, empowers system designers to make well-informed decisions aligning with budget constraints, energy objectives, and environmental sustainability goals. By striking an optimal balance between upfront costs and long-term performance, stakeholders can develop economically viable and sustainable solar energy systems, fostering the widespread adoption of renewable energy solutions.

### 7.1.1 Novelty and Contribution

Examining the previous feasibility assessments of the HESs integrated with PV tracking technologies, the research gaps that this study works on are listed below:

1. There has been no investigation on the compatibility of the HKT-based HES when it is connected to solar tracking systems.
2. The effects of albedo and  $SOC_{min}$  on operational performance, financial parameters (NPC and LCOE), and emissions rates were not studied yet.
3. Limited consideration has been drawn into project lifetime effects and technology expense of solar trackers on the cost-effectiveness of the renewable HESs.
4. Very few feasibility evaluations of renewables have taken into account the fluctuation of diesel prices and inflation rates as key financial aspects of the system's energy costs.

Hence, the primary objectives of this study encompass (i) the identification of stable and cost-effective PV tracking technologies, considering meteorological, economic, and renewable data; (ii) a comprehensive comparison of power production, reliability, emissions rates, present and energy costs; (iii) conducting a sensitivity analysis to assess the impact of fluctuating techno-economic inputs on present and energy costs; and (iv) a comparative analysis with the findings of previous research conducted in this area. Furthermore, this study contributes to the field by providing valuable insights and contributions in the following aspects:

1. Introduction of the detailed framework and comprehensive decision-making strategy for optimal sizing and feasibility analysis of HES.
2. This is the first study that investigates the feasibility of solar tracking technologies connected to HKT-based HESs in South Africa.
3. The effects of technical parameters such as albedo (ground reflectance),  $SOC_{min}$ , of battery, as well as economic parameters such as capital cost of solar trackers, on the NPC, LCOE will be investigated.

## 7.2 Methods and Materials

The research adopts a decision-making approach, serving as a comprehensive and extensive framework to guide system designers in achieving economically and technically suitable hybrid energy system (HES) designs and assessing system performance. Specifically, the proposed HES configuration integrates photovoltaic (PV), diesel generator (DG), and battery components to supply power to a rural building in South Africa. The subsequent sections present detailed information pertaining to the study's geographical locations, local resources, employed methodology, and the various energy components involved in the proposed HES.

### 7.2.1 *Demonstration of the Framework Implemented for the Optimal Design of This Study*

A thorough review of prior analyses and literature on hybrid energy systems (HES) conducted in diverse global locations has revealed a lack of a comprehensive strategic framework for HES design and planning. Addressing this gap, the present research endeavors to provide a comprehensive and systematic framework for HES design and optimization. The proposed HES framework serves as a decision-making tool to enhance the effective utilization and adaptation of HES solutions. Figure 7.2 illustrates the five key stages encompassing the paper's HES framework. In the initial stage, the primary objectives of HES investments are presented, encompassing the justification for deploying HES in commercial, industrial, and residential sectors. The framework succinctly outlines the main purposes for adopting HES, including:

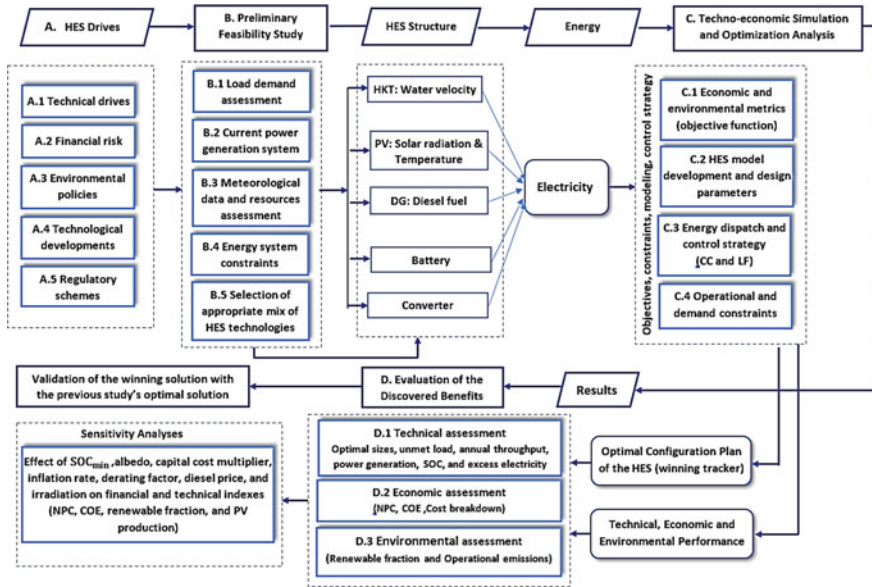


Fig. 7.2 The comprehensive procedure of optimal sizing for hybrid energy systems

1. **Technical motivation:** a suitable HES setup determines multiple technical advantages for utilities and HES users which improve power reliability and provide high-quality power.
2. **Economic challenges:** HES setup is normally installed to satisfy the required load; therefore, it offers advantages to power industry owners by reducing the costs of establishing typical centralized systems, transmission, and distribution lines, and associated infrastructure.
3. **Environmental roadmap:** maximizing the foundation and infrastructure of HES to address climate change and lowering the gas emissions toward reaching zero-emission buildings and sustainable communities.
4. **Technological advancements of components:** HES is regarded as an economical option in the current energy industry, given recent advances and huge progress in renewables and energy storage.
5. **Regulatory plans:** HES offers systems to improve the variety of power sources and boost power security.

The second stage involves conducting a preliminary feasibility analysis, which serves as a pivotal step in selecting appropriate HES technologies and determining an optimal combination to meet the load profile requirements. This stage adopts a foresight approach, necessitating a thorough evaluation of the key input parameters for HES. The primary input parameters under consideration include:

1. The activity of renewable energy resources and meteorological data.
2. Expected load profiles, main categories (residential, commercial, agricultural, etc.), and appliance consumption primarily depend on the occupant type.
3. The present power production system meets load profiles.
4. Energy system constraints related to the HES components can restrict or prohibit the use of some energy options, such as geographic constraints (e.g., merely some area is applicable for the installation of solar panels or challenges limiting the durability of wind turbine foundations) [41]

Once the energy generation options have been identified, the next step involves establishing the most effective controlling strategy. This decision is crucial in optimizing the system and addressing existing challenges. Given the paramount importance of financial considerations in electrification plans, the optimization framework incorporates various HES economic metrics to determine the most suitable solution. Depending on the specific context, such as energy components, geographical data, and financial and technical characteristics, cycle charging (CC) and load following (LF) dispatch strategies emerge as promising methods to significantly reduce cost indexes. Moving to the third step, a comprehensive techno-economic design and optimization study (stage C) becomes essential. This involves accurately defining the technical and economic parameters of the energy solutions to avoid incorrect component sizing. To ensure reliability, an appropriate operational and optimization plan must be maintained, supported by a reliable economic investigator. Consequently, the proposed optimized HES is evaluated simultaneously for its operational, economic, and environmental characteristics. Step D specifies which parameters under technical, economic, and environmental viewpoints will be evaluated. Additionally, conducting sensitivity analysis is crucial to generalize results under varying technological, economic, and climatic conditions. The following sections delve into the implementation of techno-economic optimization and sensitivity evaluations.

### 7.3 The Intended Site Description

Figure 7.3 depicts a rural family in a distant region of Kwazulu Natal province, South Africa. This place enjoys a humid environment with a geographical elevation of 1,169 m above sea level. The annual building load profile is depicted in Fig. 7.4, which was acquired from Ref. [42], residential power tends to be procured for equipment such as fridges, TV, lights, kettle, toaster, iron, cell phone chargers, etc., with an annual load of 38 kWh/day.





Fig. 7.3 The map of the rural place located in South Africa

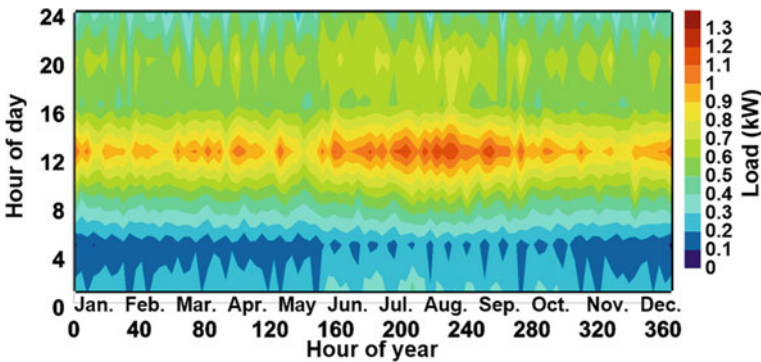


Fig. 7.4 The annual electrical load of the residential place

### 7.3.1 Renewable Resources

Figure 7.5 depicts the water velocity and solar irradiation from the sun at the intended place. NASA [43] and an experimental investigation in this vicinity [44] provided the monthly data. In comparison to most other places in the globe, irradiation from the sun in the summer fluctuates between 3.5 to 5.5 kWh/m<sup>2</sup>/day. The highest and lowest irradiation is observed in December and June, respectively. The decrease in solar irradiance in the summer period can be attributed to factors such as seasonal variation in sun angle, weather patterns and cloud cover, regional climate, and the impact on solar energy systems in this area. The average monthly water velocity profile confirms that the hydrokinetic turbine would produce the highest energy

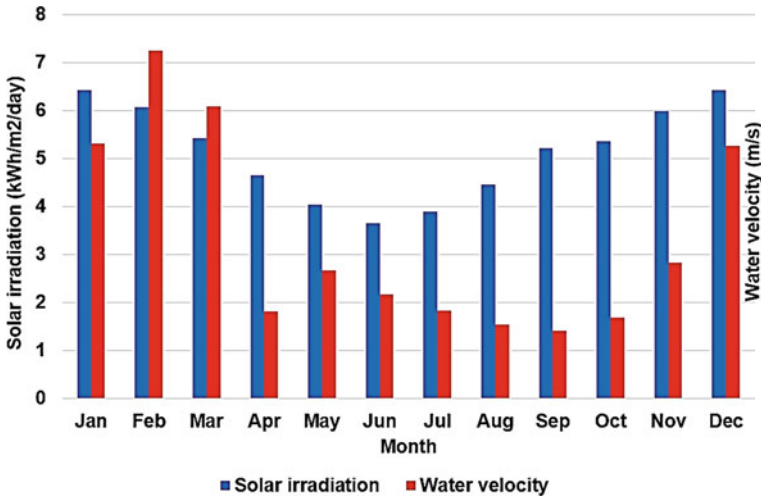


Fig. 7.5 Representation of monthly a water speed and b solar irradiation [51]

yield in the fall and winter since these are the months with the most accessible water velocities.

## 7.4 Specification of the HES

In Fig. 7.6, the schematic layout of grid-independent energy systems is depicted, consisting of a photovoltaic system and its converter, a diesel generator, and a hydrokinetic turbine, all directly connected to the AC bus. Additionally, batteries are integrated into the system, linked to the AC through an AC/DC bidirectional converter to facilitate power-sharing. Table 7.2 presents the financial attributes and expected lifetime of each energy production component.

### 7.4.1 Diesel Generator

Diesel generators in off-grid solutions satisfy the electrical load first, which reduces the reliance on batteries, resulting in cost—savings. The generator efficiency is shown in the formula below [50]:

$$\eta_{DG} = \frac{3.6P_{DG}}{GHC.LHV_D} \quad (7.1)$$

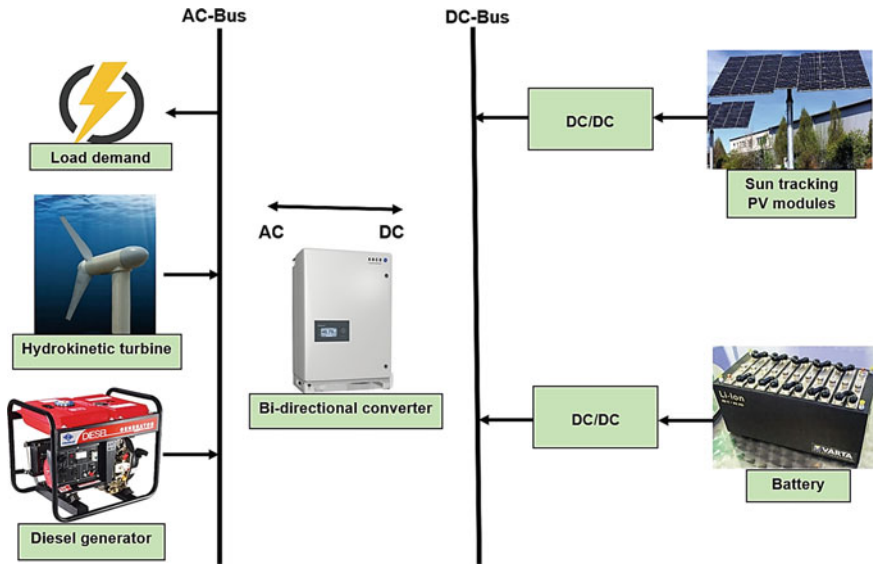


Fig. 7.6 The intended hybrid energy solution of the schematic configuration

Table 7.2 Financial description of the energy components

Cost type	Energy component				
	PV system	Diesel generator	Hydrokinetic turbine	Battery	Converter
Capital expense (\$/kW)	550	350	1,300	200/kWh	300
Replacement expense (\$/kW)	550	325	870	180/kWh	300
Lifetime (yr)	25	20	15	15	15
Reference	[45]	[46]	[47]	[48]	[49]

where  $\eta_{DG}$ ,  $\rho_f$ , and  $P_{DG}$  stands for the generator efficiency (%), the output power (kW), the fuel density ( $\text{kg/m}^3$ ), and the rated generator power (kW), respectively. The hourly generator’s fuel consumption (L/h) is shown in the following equation [49]:

$$\dot{m}_{\text{fuel}} = F_0 Y_{DG} + F_1 P_{DG} \tag{7.2}$$

$Y_{DG}$  is the generator’s rated capacity in this equation (kW),  $F_0$  is the intercept co-efficient of the generator fuel curve (L/h/rated kW or  $\text{m}^3/\text{h}/\text{rated kW}$ ), and  $F_1$  is the fuel curve slope (L/h/output kW or  $\text{m}^3/\text{h}/\text{output kW}$ ).

## 7.4.2 PV System

The effectiveness of solar panels varies depending on the surroundings (temperature in the environment, moisture, and so on), solar irradiation ( $\text{kWh}/\text{m}^2/\text{day}$ ), and technology for collectors. To compute the PV module's output power, use the formula given [51]

Where  $W_{\text{pv}}$  is the PV array's peak power output (kW),  $f_{\text{pv}}$  is the PV derating factor (%), the current hour's solar irradiance is denoted by  $G_{\text{T}}$  ( $\text{kW}/\text{m}^2$ ), The incident radiation at standard test settings is denoted by  $G_{\text{S}}$  ( $1 \text{ kW}/\text{m}^2$ ),  $\alpha_p$  is the temperature coefficient ( $\%/^{\circ}\text{C}$ ).  $T_{\text{C}}$  stands for the PV module temperature in degrees Celsius ( $^{\circ}\text{C}$ ) and  $T_{\text{S}}$  stands for the PV module temperature in the test condition in degrees Celsius ( $^{\circ}\text{C}$ ).

### 7.4.2.1 Solar PV Tracking System Technologies

PV tracking mechanism is utilized to adjust PV modules toward the sun's rays to enhance the PV modules' efficiency and productivity by maximum utilization of solar irradiance. Fixed-tilt solar PV modules typically employ manually adjustable panel slopes for simplicity and cost-effectiveness. The PV system is situated at a fixed slope, and azimuth suffers from a considerable deficiency in solar irradiation as a result of the sun passing through the day and its orbit fluctuating annually [29]. Sun-tracking PV systems typically can be constantly adaptable toward high-density rays from the sun. The followings are the main PV tracking methods and corresponding scenarios applied in this analysis:

1. **Scenario I:** Horizontal-axis monthly adjustment (HM). Each month, the tilt angle is changed to ensure that the panels at noon are at almost a perpendicular angle to the sun's beams while the rotating axis circulates around the horizontal (east–west) axis.
2. **Scenario II:** Horizontal-axis continuous adjustment (HC). The tilt angle is unceasingly altered while the rotation is around the horizontal.
3. **Scenario III:** Vertical-Axis continuous adjustment (VC). The tilt is fixed, but the PV panel rotates infinitely around the vertical (north–south) axis.
4. **Scenario IV:** Dual-axis-tracker (DT). To keep a perpendicular angle between PV arrays and sun beams, the PV panels continuously spin in both directions (horizontal and vertical).

These PV tracking technologies are classified based on how many rotational axes they have, as shown in Fig. 7.7.

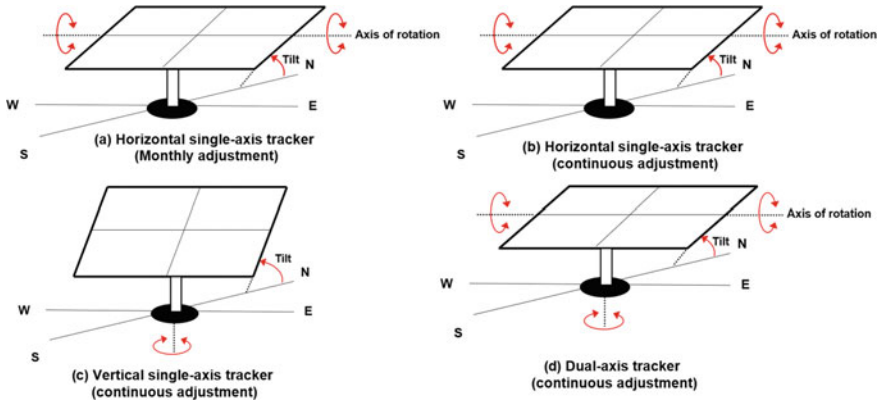


Fig. 7.7 Illustration of investigated tracking systems

### 7.4.3 Hydrokinetic Turbines

The water’s velocity affects the features of hydrokinetic turbines. The longitudinal system absorbs the energy from the waves to create energy (which is placed vertically in the direction of the waves in the water). 3 Hydraulic systems positioned inside the device’s joints turn the energy into electricity. Then, using proprietary units and cables, the energy generated is converted to shore power. The largest amount of energy available from sea waves can be seen in the equation below [52].

$$P_{max} = \frac{\rho g^2 T H^2}{64\pi} \times L_{max} \tag{7.4}$$

The maximum available power is  $P_{max}$  in this case,  $\rho$  is the water density,  $g$  is the gravitational acceleration,  $T$  is the wave period, The important wave height is indicated by the symbol  $H$ , and  $L_{max}$  is the maximum power absorption width.

### 7.4.4 Battery Storage

Li-ion batteries are regarded as a backup because of their dependability, affordable efficiency, high depth of discharge (DOD), and adaptable technology. It aids HES in distributing and preserving energy generated by components so that it can be used in times of uncertainty. Equation (7.5) [53] can be used to estimate the amount of stored energy.

$$P_{Batt,Cmax} = \frac{\min(P_{Batt,Cmax,kbm} P_{Batt,Cmax,mcr} P_{Batt,Cmax,mcc})}{\eta_{Batt,C}} \tag{7.5}$$

In this case,  $\eta_{\text{Batt,C}}$  is the efficiency of charge storage,

$$P_{\text{Batt,Cmax, kbm}} = \frac{kQ_1 e^{-k\Delta t} + Qkc(1 - e^{-k\Delta t})}{1 - e^{-k\Delta t} + c(k\Delta t - 1 + e^{-k\Delta t})} \quad (7.6)$$

$$P_{\text{Batt,Cmax, mcr}} = \frac{(1 - e^{-\alpha_c \Delta t})(Q_{\text{max}} - Q)}{\Delta t} \quad (7.7)$$

$$P_{\text{Batt,Cmax, mcc}} = \frac{N_{\text{Batt}} \cdot I_{\text{max}} \cdot V_{\text{nom}}}{1000} \quad (7.8)$$

The constant of storage rate,  $k(\text{h}^{-1})$ , is used here, at the first timestep,  $Q_1$  represents the amount of energy that was still available. (kWh),  $\Delta t$  is time step duration (h), The amount of energy stored in the batteries is denoted by  $Q$  at the initial stage (kWh),  $c$  is the ratio of storage capacity,  $\alpha_c$  is the maximum charge of the battery (A/Ah),  $Q_{\text{max}}$  is the total capacity of storage (kWh),  $N_{\text{Batt}}$  is the quantity of batteries,  $I_{\text{max}}$  is the battery's maximum battery current (A), and  $V_{\text{nom}}$  is the battery's nominal voltage.

### 7.4.5 Converter

To harmonize hybrid energy systems, the system converter is crucial. The main function of a converter is to keep energy flowing between AC and DC. It acts as a medium for converting DC to AC electric power and connects the two systems converting DC to AC. The converters' power rating is derived using Eq. (7.9) [51]:

$$P_{\text{inv}}(t) = \left(\frac{\rho}{\rho_0}\right) \cdot P_{\text{max.L}}(t) / \eta_{\text{inv}} \quad (7.9)$$

where  $P_{\text{max.L}}$  is the maximum load demand, and inverter efficiency is defined as  $\eta_{\text{inv}}$ .

### 7.4.6 Financial Equations

The total cost, consisting of initial, replacement, operation, and maintenance (O&M), and fuel costs, minus the project's salvage cost at the end of its life, is expressed as the net present cost (NPC). Equation (7.10) can be used to get the total NPC [14]

$$C_{\text{npc,tot}} = \frac{C_{\text{ann,tot}}}{\text{CRF}(i, R_{\text{proj}})} \quad (7.10)$$

where  $C_{\text{ann,tot}}$  represents the total annual cost (\$/year), the yearly real interest rate is symbolized by the letter  $i$  (%), The TP signifies the project's lifetime (year), and

CRF stands for element of capital recovery, This is measured utilizing the equation below [40]:

$$\text{CRF}(i, n) = \frac{i(1+i)^n}{(1+i)^n - 1} \quad (7.11)$$

The project's lifetime (year) is represented by  $n$ , and  $i$  is the annual interest rate, which is computed using the equation [19]:

$$i = \frac{i - f}{1 + f} \quad (7.12)$$

where the rate of yearly inflation is (%).

Levelized cost of energy (LCOE): among the most significant measures for evaluating HES's cost-effectiveness. The LCOE is calculated by dividing the average HES cost by the total electrical energy served (kWh), which is measured by Eq. (7.13) [54]:

$$\text{LCOE} = \frac{C_{\text{ann,tot}}}{L_{\text{ann,load}}} \quad (7.13)$$

Here,  $L_{\text{ann,load}}$  is the overall yearly electrical consumption (kWh/year), and  $C_{\text{ann,tot}}$  is the total annual expense (\$/year).

## 7.5 Results and Discussion

The technical, environmental, and financial results of the winning energy systems are explained in this part and then will be complemented with the sensitivity assessment and a more detailed examination of each target area.

### 7.5.1 The Outcomes of the System Optimization

HOMER simulates hybrid energy alternatives, and solutions that are not practical (those that fail to meet the user-specified restrictions) will be excluded from the final optimization outcomes and not exhibited. The NPC and LCOE determine how the feasible options are ordered. Table 7.3 presents the technical and financial results of HESs and the considered tracking technologies. The results show that using a VC tracker integrated into DG/PV/HKT results in the least NPC of \$13.70 k. LCOE of this solution also is \$0.058/kWh less than PV/HKT hybrid system. Implementing a PV/HKT system with a VC tracker reveals the most appropriate option in electricity production. The average of surplus electricity and the capacity shortage is observed

to be higher amongst PV/HKT options. The breakdown of the associated expenses in tracker-based optimal scenarios is shown in Fig. 7.8. The majority of the total expenses are dedicated to the initial cost of the components. Moreover, the optimal HV-based HES achieves a \$1.52k, \$0.55k, and \$0.41k higher capital cost than optimal HESs under VC, HM, and DA, respectively. Under the DA tracker, fuel usage and replacement costs are found to be higher than in other cases.

Using DG to produce electricity is damaging to the environment since the burning of diesel produces gaseous pollutants. Gas emissions, including CO<sub>2</sub>, NO<sub>x</sub>, PM, UHC, SO<sub>2</sub>, and CO, are among the pollutants released from diesel generator [55]. Table 7.4 compares the total GHG emissions emitted by the winning energy source using different solar tracking systems from an environmental standpoint. The VC-based option is the most environmentally friendly alternative as compared with other options, emitting the lowest CO<sub>2</sub> level (282 kg/year). Emissions rates from HESs connected to HM and HC trackers are roughly similar.

### 7.5.2 Techno-Economic Analysis of the Energy Solutions

It is crucial to examine the major financial metrics and power production profiles for optimal HES under each PV tracker. Table 7.5 illustrates the electrical outputs of each component under the integration of intended PV trackers. As per the table, the energy costs of the DG in all tracker options are measured at \$0.273/kWh, which is comparable to HKT (0.0213 \$/kWh). The greatest energy cost from the PV is seen under the HM tracker system at \$0.075/kWh. The least energy costs of PV generation compared with HKT and DG indicate the desirably economical implementation of PV systems in South Africa.

The term “unmet electric load” refers to the portion of the load that remains unsatisfied due to insufficient energy output. Depending on the magnitude of the unmet electric load and renewable fraction, adjustments can be made to the PV size, either increasing or reducing it accordingly. Moreover, the concept of storage throughput (kWh/year) is introduced, representing the total energy flow passing through the battery units annually. The average energy between the incoming and outgoing energy is utilized to calculate the battery throughput, which provides insights into the battery’s operational lifespan. Notably, there exists an indirect relationship between the annual throughput and the battery’s lifetime. As depicted in Fig. 7.9, all the considered options exhibit unmet loads, implying varying levels of reliability in meeting the required load. Among these options, the VC-based DG/PV/HKT configuration and the HC-based hybrid PV/HKT option demonstrate higher reliability due to their lowest unmet loads. Conversely, configurations involving DA trackers exhibit lower reliability in fulfilling the load for both scenarios.

Figures 7.10 and 7.11 illustrate the annual profile of the battery state of charge (SOC) and its relative frequency for the selected winning tracking technology (VC). Throughout the year, with the exception of December, the lowest SOC values are predominantly observed from the beginning of fall to the end of April. This decline



**Table 7.3** Results of the optimal hybrid energy systems under the integration of different tracking technologies

Components	Tracker	Controller	NPC	LCOE	PV	DG	HKT	CNV	BT	Electricity produced	Excess electricity
DG/PV/HKT	VC	LF	13.70	0.258	3.05	2	1	6	2.12	7.36	1.98
	HM	LF	15.04	0.283	2.5	2	1	6	2	8.65	2.27
	HC	LF	15.6	0.293	2.3	2	1	6	2.01	9.52	3.15
	DA	LF	16.21	0.286	1.8	2	1	6	2.18	10.4	4.02
PV/HKT	VC	CC	16.8	0.316	5.65	-	1	13	2.9	9.3	5.1
	HM	CC	19.45	0.366	4.5	-	1	16	2.86	10.11	5.44
	HC	CC	20.9	0.393	4.6	-	1	6	2.71	10.88	5.8
	DA	CC	21.18	0.399	4.2	-	1	16	3.48	11.29	6.91

\* PV = Photovoltaic system, DG = diesel generator, HKT = hydrokinetic turbine, CNV = converter, BT = battery

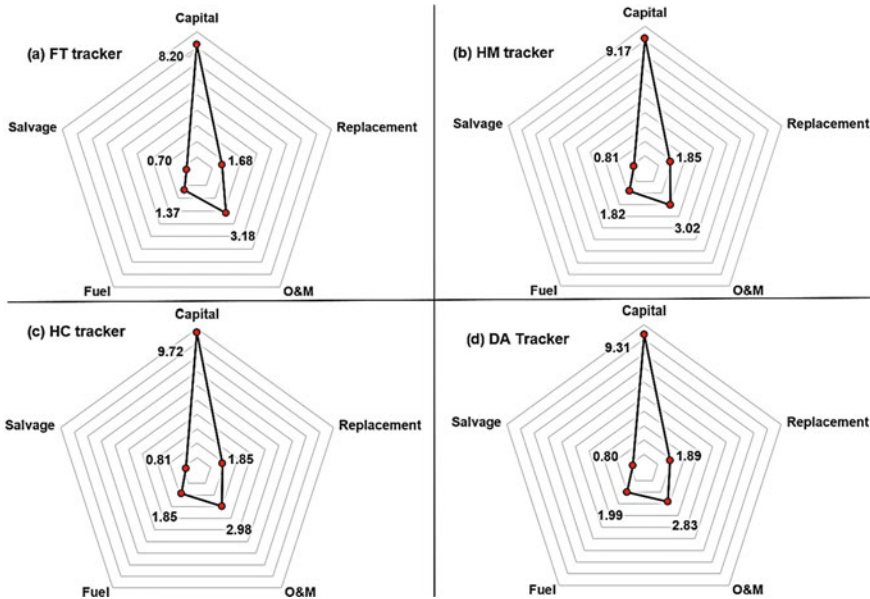


Fig. 7.8 Cost breakdown of each tracker technology connected to the HES

Table 7.4 Breakdown of the emission rates from the tacker-based scenarios

Gas type	Tracking configuration			
	FC	HM	HC	DA
CO <sub>2</sub> (carbon dioxide)	277	369	375	404
CO (carbon monoxide)	1.7	2.3	2.3	2.5
UHC (unburned hydrocarbon)	0.076	0.10	0.10	0.11
PM (particulate matter)	0.010	0.013	0.014	0.015
SO <sub>2</sub> (sulphur dioxide)	0.6	0.9	0.9	0.9
NO <sub>x</sub> (nitrogen oxide)	1.6	2.1	2.2	2.3
Total yearly emissions (kg/year)	282	374.4	380.5	410

in SOC can be attributed to the limited and unstable solar irradiation during this period. On the other hand, the SOC levels tend to fluctuate around 58.4% and 100% for approximately 68% of the time each year, indicating that the batteries are mostly operating in a “shallow” discharge state during the majority of the year. This finding suggests that the batteries are adequately charged and capable of meeting the energy demands effectively for a significant portion of the year.

The occurrence of excess electricity results from a discrepancy between energy production and the duration of consumption. As depicted in Figs. 7.12 and 7.13, the surplus energy is mainly generated between 10:00 a.m. and 5:00 p.m., with the peak of extra power observed around noon due to the higher PV output during that period.

**Table 7.5** Presentation of the component outputs in considered tracking technologies

	PV production	HKT production	HKT production	DG production
VC	<p>Yearly production: 5,030 kWh/year Equipment energy cost: \$0.042/kWh</p>	<p>Yearly production: 2,075 kWh/year Equipment energy cost: \$0.215/kWh</p>	<p>Yearly production: 270 kWh/year Equipment energy cost: \$0.275/kWh</p>	
HM	<p>Yearly production: 4,235 kWh/year Equipment energy cost: \$0.063/kWh</p>	<p>Yearly production: 2,085 kWh/year Equipment energy cost: \$0.213/kWh</p>	<p>Yearly production: 360 kWh/year Equipment energy cost: \$0.273/kWh</p>	

(continued)

Table 7.5 (continued)

	PV production	HKT production	DG production
HC	<p>Yearly production: 4,102 kWh/year Equipment energy cost: \$0.075/kWh</p>	<p>Yearly production: 2,082 kWh/year Equipment energy cost: \$0.213/kWh</p>	<p>Yearly production: 372 kWh/year Equipment energy cost: \$0.273/kWh</p>
DA	<p>Yearly production: 3,895 kWh/year Equipment energy cost: \$0.068/kWh</p>	<p>Yearly production: 2,073 kWh/year Equipment energy cost: \$0.215/kWh</p>	<p>Yearly production: 402 kWh/year Equipment energy cost: \$0.275/kWh</p>

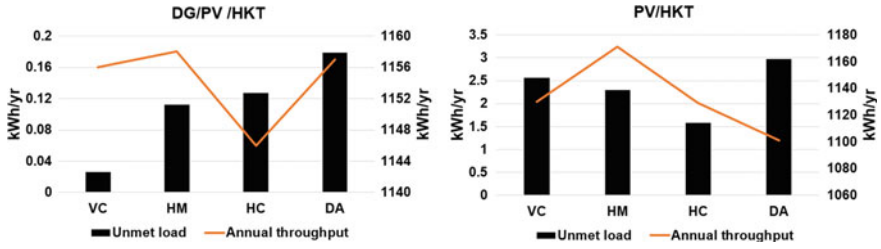


Fig. 7.9 Comparison of unmet load and annual throughput

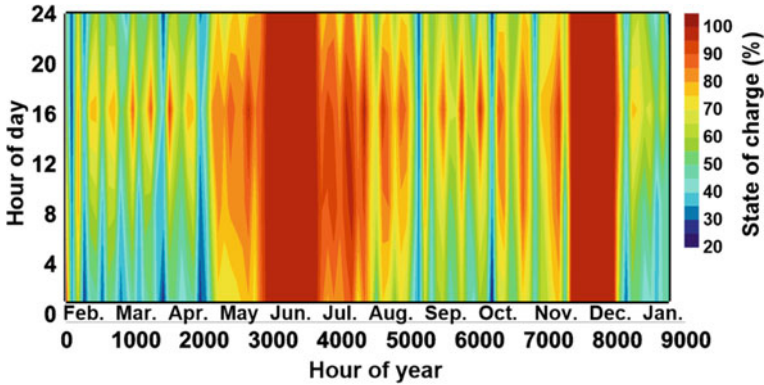


Fig. 7.10 Yearly profile of the battery state of charge (SOC) under the winning system

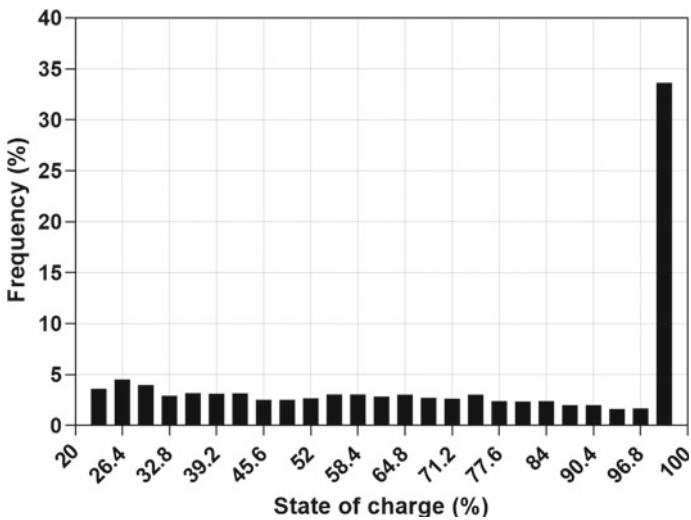


Fig. 7.11 Relative frequency for the SOC under the winning option

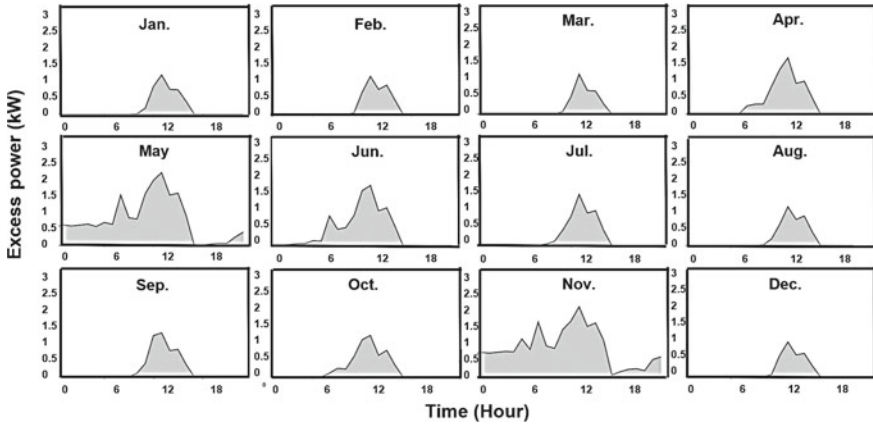


Fig. 7.12 Monthly average variation of excess power in the winning case

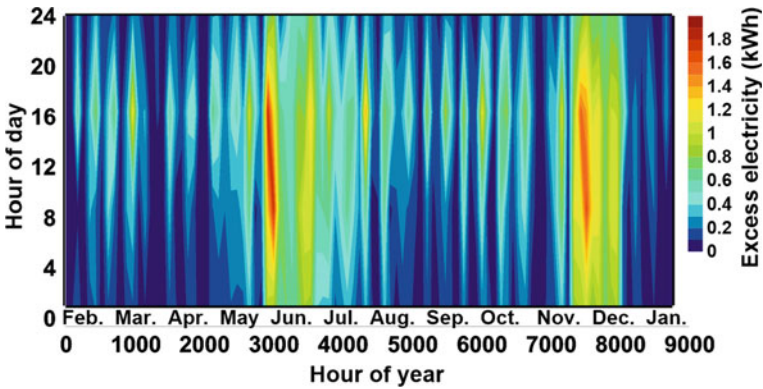


Fig. 7.13 Hourly profile of excess power in the winning case

While the selected HES with VC tracker effectively meets the energy requirements of the site, it is worth noting that during the months of February to May and August to November, it is not the most opportune time to fully charge the batteries. This is likely due to the relatively lower availability of excess electricity during these time periods, which affects the ability to maximize battery charging.

### 7.5.3 Sensitivity Evaluation

The sensitivity assessment of the winning case is shown in this part. This analysis allows predicting how the energy option would change under various technical and economic circumstances.  $SOC_{min}$  is the lowest magnitude of battery charging status

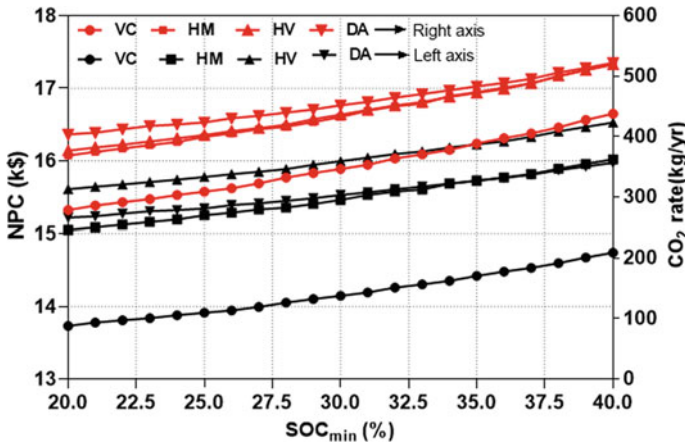


Fig. 7.14 Impacts of SOC<sub>min</sub> on NPC and CO<sub>2</sub> in various scenarios

below which the battery is never discharged. To prevent the battery bank from being damaged by excessive discharge, the SOC<sub>min</sub> has not been tuned to a very low amount [56]. Figure 7.14 shows the impacts of the SOC<sub>min</sub> fluctuation on NPC and CO<sub>2</sub> production. An increase in SOC<sub>min</sub> leads to growth in NPC and CO<sub>2</sub> production of all tracking technologies. The most significant impact is seen under the VC tracker; a 20% increase in SOC<sub>min</sub> value will increase NPC and CO<sub>2</sub> by \$0.17k and 1.1 t/yr, respectively. As the VC tracker is not able to receive intense irradiation compared to other tracking devices, it will be more reliant on the diesel generator. An increment in SOC<sub>min</sub> would increase the DG’s reliance on it to meet the required load, and then higher O&M expenses, which leads to increasing NPC and CO<sub>2</sub> levels.

Albedo refers to the capacity of an object or surface to reflect light from the sun. As per the meteorological conditions in the case area, the ground cover is potentially snow or rain as well as grass in winter and summer, respectively. As a consequence, the impacts of albedo fluctuation on PV performance and its corresponding expenses are explored in this study. The capacity of an object to reflect light from the sun is known as “albedo.” The change of ground reflectance against PV generation and the renewable fraction is depicted in Fig. 7.15. Increased albedo enhances solar irradiation on PV arrays, which results in PV output and renewable fraction. The VC-based and HM-based energy systems show the greatest increase in PV production and RF values. Figure 7.16 represents the variation of albedo on the NPC and LCOE for each hybrid solution. The albedo increase would decrease the required PV size leading to lower NPC and LCOE. The highest reduction in NPC and LCOE is observed under DA-based cases, Fig. 7.17 illustrates how the energy cost of the unit varies when the capital cost of tracking equipment changes. The expense of the DA tracker should decrease by a minimum of 35% in order for the resultant to be comparable to that of HV with the initial value.

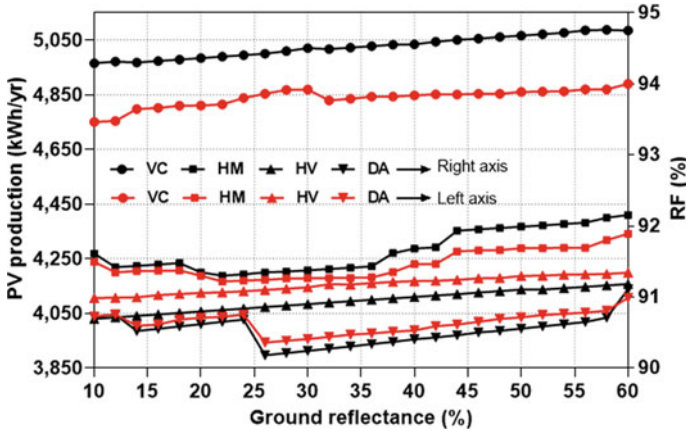


Fig. 7.15 The impact of albedo on PV production and renewable penetration of the considered tracking technologies

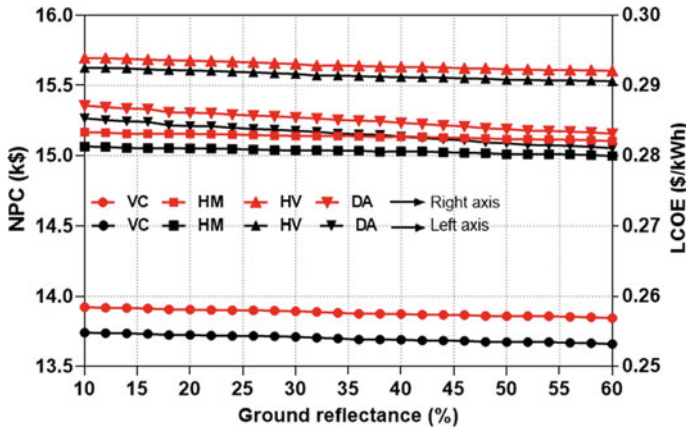


Fig. 7.16 The impact of albedo on NPC and LCOE of the considered tracking technologies

Derating factor of PV panels is another studied sensitivity variable in this section. It accounts for a decrease in PV output due to actual conditions such as shading, aging, dust cover, wire losses, and snow. Derating factor in this research study was set at 80%. Figure 7.18a and b demonstrate how the derating factor and capital cost of PV panels affect the profitability of the selected energy solutions. The lowest NPC and LCOE are found when the PV initial cost is lower and the derating factor is higher, respectively. An increase in the capital cost of PV system by 2.5 times in the constant derating factor would increase NPC and LCOE by \$4.8k and 0.1/kWh, respectively. Project lifetime also is observed as an important indicator in the economic analysis of renewable HES. Figure 7.19a and b show how LCOE is



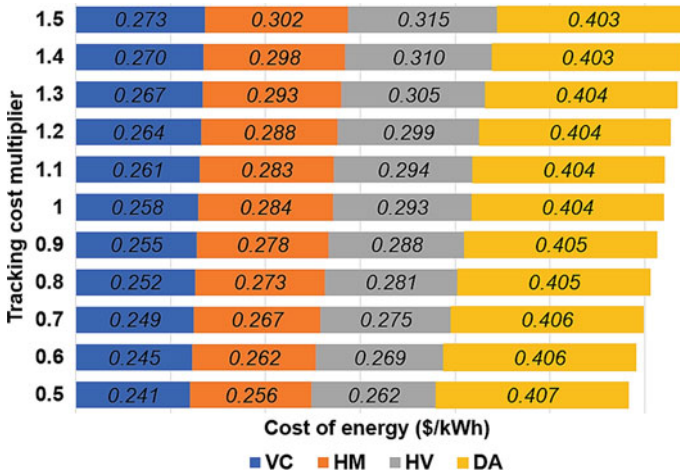


Fig. 7.17 Fluctuation of initial costs of PV trackers against the COE

sensitive to solar irradiation fluctuation in short-term (10 years) and long-term (20 years) project lifetimes. The higher the solar irradiation, the greater PV output can be obtained, resulting in lowering overall energy costs and NPC. The conclusion can be that renewable HES can have more resource values and lower energy costs as the project lifetime increases.

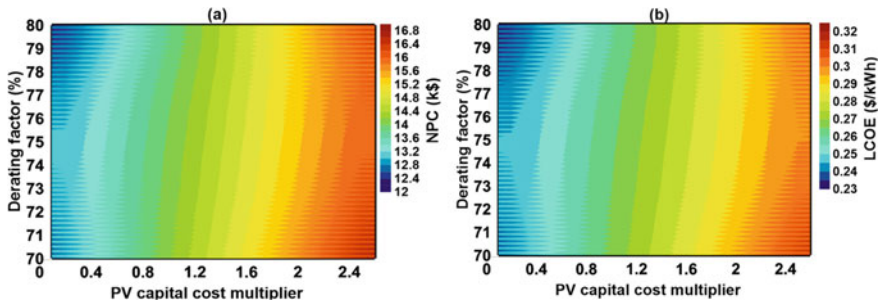


Fig. 7.18 Effect of PV capital cost multiplier and derating factor on a NPC and b LCOE

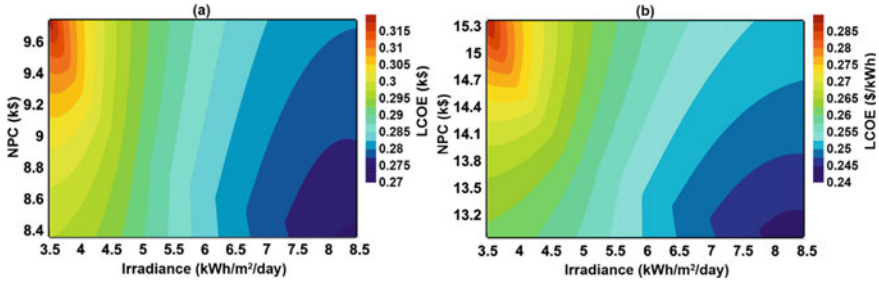


Fig. 7.19 Effect of solar irradiation on LCOE during **a** short-term and **b** long-term project

### 7.5.4 Comparison & Validation

A comparative analysis between the findings of this present study and previously conducted research in the same domain reveals insights into the promising or unprofitable future of the selected hybrid energy options. However, conducting a direct comparison between the current study and prior works presents challenges due to variations in the hybrid energy system (HES) configuration, technology choices, component sizes, and financial parameters. Nonetheless, the results of the optimal solutions in this study, as depicted in Fig. 7.20, demonstrate a more favorable outcome with a lower net present cost (NPC) and levelized cost of energy (LCOE) by \$58k, and \$0.005/kWh, respectively, compared to the previous research. The earlier study exhibited higher excess electricity, which could potentially be utilized to charge the battery and enhance the reliability of the current optimal solution. Moreover, the analysis in the current study reveals that battery autonomy, defined as the ratio of battery size to electric load, is approximately five times greater than that observed in the previous research. Furthermore, the comparison between the optimal tracking technology employed in the current study and that of the earlier research holds significant importance in validating the practicality and profitability of the chosen technology. While the net present cost (NPC) can vary considerably based on factors such as local tracker prices, energy component costs, required load, and renewable resource availability, it may not serve as a precise indicator for direct comparison. Instead, presenting the optimal trackers and comparing the NPC growth rates of various tracking systems can offer a suitable method to guide consumers toward selecting the most financially and performance-appropriate tracker. Table 7.6 presents the breakdown of the optimal solution and economic parameters of the previous findings which were assessed on different solar tracker technologies. Consistent with other studies akin to the current research, vertical-axis PV trackers (VC) have been identified as favorable solutions due to their cost-effectiveness and reliability. Additionally, the DA tracking technology exhibited higher NPC growth rates across various scenarios.

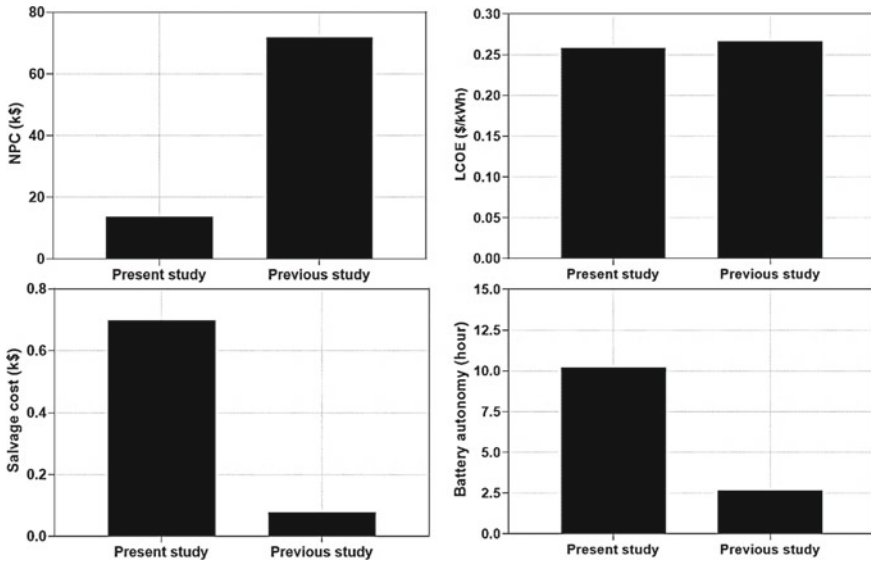


Fig. 7.20 Comparison of the results in the present and previous study

Table 7.6 Comparison of the present results with the literature findings

	Ref., location	HES <sup>1</sup>	Winning tracker <sup>2</sup>	NPC growth rate (%) <sup>3</sup>			
				HM	HC	VC	DT
Grid-connected	[29], Makkah, Saudi Arabia	PV	DA	20.63	20.00	1.00	19.95
	[57], Eight cities in Iran	PV	VC	2.06	3.40	Optimal	0.70
	[39], Alkharj City, Saudi Arabia	PV/ELC/FC	VC	–	78.00	Optimal	84.00
Off-grid	[34], Hilly terrain, India	PV/WT	VC	2.00	3.86	Optimal	9.77
	[58], South of Iran	PV/Pump storage hydroelectric	DA	–	12.9	–	Optimal
	[37], Healthcare facility, India	PV	VC	7.60	16.40	Optimal	13.90
	Kwazulu Natal Province, South Africa	PV/DG/HKT	VC	9.80	13.80	Optimal	18.30

## 7.6 Conclusion

This study aimed to determine the most stable and profitable hybrid renewable energy alternative using four PV tracking technologies for a residential place in South Africa. The optimal sizing of the hybrid energy solutions consisting of DG, PV system, HKT, battery, and converter was conducted to ascertain the reliable and cost-effective solution. The winning or optimal energy system was selected as per its lowest NPC and LCOE. A combination of DG, PV, and HKT under the VC tracker achieved the most desirable hybrid energy system in terms of cost-effectiveness. The NPC and LCOE for this option, which included 2 kW DG, 3.02 kW PV, 1 HKT, 6 battery units, and 2.12 kW converter, were \$13.7k, \$0.258/kWh, and 281.11 kg/year, respectively. The use of PV/HKT system with VC tracker showed the most appropriate option for electricity production. The highest and lowest CO<sub>2</sub> emissions were observed in HES connected to the FT and DA tracking technologies, respectively. The VC-based DG/PV/HKT option and the HC-based hybrid PV/HKT option are regarded as the most dependable due to their lowest unmet loads. Conversely, DA trackers with both configurations achieve lower reliability to meet the required load. A sensitivity evaluation was performed in the next section to predict how the renewable energy options and PV trackers would change under various technical and economic circumstances. As per the sensitivity analysis on tracking configurations, the VC strategy is more sensitive to the fluctuation of SOC<sub>min</sub>; rising SOC<sub>min</sub> will increase NPC and CO<sub>2</sub> by \$0.16k and 1.08 tonnes/year, respectively. Furthermore, VC-based and HM-based hybrid systems show the greatest increase in PV production and RF due to increasing albedo.

## 7.7 Future Studies

In the future research attempt, a comprehensive life cycle analysis (LCA) can be conducted to assess the environmental impact of solar tracking technologies and the overall renewable energy system over their entire lifecycle. This potential analysis can consider various stages, including manufacturing, installation, operation, and end-of-life. The combination of techno-economic analysis and life cycle cost analysis (LCA) provides a comprehensive assessment of both the financial and environmental aspects of a project. The techno-economic analysis evaluates the financial viability and feasibility by considering capital costs, revenue streams, and payback periods. On the other hand, LCA assesses the total cost of the project over its entire lifecycle, including environmental impacts and energy consumption. Integrating these analyses allows decision-makers to make more informed and balanced choices, considering both economic benefits and environmental implications. This approach leads to the development of sustainable and financially viable solutions that align with both economic and environmental goals, enabling better decision-making and resource allocation.

## References

1. J.G. Peña Balderrama et al., Incorporating high-resolution demand and techno-economic optimization to evaluate micro-grids into the Open Source Spatial Electrification Tool (OnSSET). *Energy Sustain. Dev.* **56**, 98–118 (2020). <https://doi.org/10.1016/j.esd.2020.02.009>
2. T. Kobayakawa, T.C. Kandpal, A techno-economic optimization of decentralized renewable energy systems: trade-off between financial viability and affordability—a case study of rural India. *Energy Sustain. Dev.* **23**, 92–98 (2014). <https://doi.org/10.1016/j.esd.2014.07.007>
3. T. Levin, V.M. Thomas, Can developing countries leapfrog the centralized electrification paradigm? *Energy Sustain. Dev.* **31**, 97–107 (2016). <https://doi.org/10.1016/j.esd.2015.12.005>
4. M. Babaei Jamnani, A. Kardgar, Energy-exergy performance assessment with optimization guidance for the components of the 396-MW combined-cycle power plant. *Energy Sci. Eng.* **8**(10), 3561–3574 (2020). <https://doi.org/10.1002/ese3.764>
5. T.S. Costa, M.G. Villalva, Technical evaluation of a PV-diesel hybrid system with energy storage: case study in the Tapajós-Arapiuns extractive reserve, Amazon, Brazil. *Energies* **13**(11), 2969 (2020). <https://doi.org/10.3390/en13112969>
6. X. Liu, Q. Tan, Y. Niu, R. Babaei, Techno-economic analysis of solar tracker-based hybrid energy systems in a rural residential building: a case study in South Africa. *Int. J. Green Energy* **20**(2), 192–211 (2023). <https://doi.org/10.1080/15435075.2021.2024545>
7. J. Lata-García, F. Jurado, L.M. Fernández-Ramírez, H. Sánchez-Sainz, Optimal hydrokinetic turbine location and techno-economic analysis of a hybrid system based on photovoltaic/hydrokinetic/hydrogen/battery. *Energy* **159**, 611–620 (2018). <https://doi.org/10.1016/j.energy.2018.06.183>
8. H.J. Vermaak, Techno-economic analysis of solar tracking systems in South Africa. *Energy Procedia* **61**, 2435–2438 (2014). <https://doi.org/10.1016/j.egypro.2014.12.018>
9. K. Kusakana, Optimization of the daily operation of a hydrokinetic–diesel hybrid system with pumped hydro storage. *Energy Convers. Manag.* **106**, 901–910 (2015). <https://doi.org/10.1016/j.enconman.2015.10.021>
10. K. Kusakana, Optimal operation scheduling of a hydrokinetic–diesel hybrid system with pumped hydro storage, in *2015 4th International Conference on Electric Power and Energy Conversion Systems (EPECS)*, (2015), pp. 1–6. <https://doi.org/10.1109/EPECS.2015.7368539>
11. M. Shafiey Dehaj, H. Hajabdollahi, Multi-objective optimization of hybrid solar/wind/diesel/battery system for different climates of Iran. *Environ. Dev. Sustain.* **23**(7), 10910–10936 (2021). <https://doi.org/10.1007/s10668-020-01094-1>
12. M. Najafi Ashtiani, A. Toopshekan, F. Razi Astaraei, H. Yousefi, A. Maleki, Techno-economic analysis of a grid-connected PV/battery system using the teaching-learning-based optimization algorithm. *Sol. Energy* **203**, 69–82 (2020). <https://doi.org/10.1016/j.solener.2020.04.007>
13. S.A. Mousavi, R.A. Zarchi, F.R. Astaraei, R. Ghasempour, F.M. Khaninezhad, Decision-making between renewable energy configurations and grid extension to simultaneously supply electrical power and fresh water in remote villages for five different climate zones. *J. Clean. Prod.* **279**, 123617 (2021). <https://doi.org/10.1016/j.jclepro.2020.123617>
14. R. Babaei, D.S. Ting, R. Carriveau, Feasibility and optimal sizing analysis of stand-alone hybrid energy systems coupled with various battery technologies: a case study of Pelee Island. *Energy Rep.* **8**, 4747–4762 (2022). <https://doi.org/10.1016/j.egy.2022.03.133>
15. S. Vendoti, M. Muralidhar, R. Kiranmayi, Techno-economic analysis of off-grid solar/wind/biogas/biomass/fuel cell/battery system for electrification in a cluster of villages by HOMER software. *Environ. Dev. Sustain.* **23**(1), 351–372 (2021). <https://doi.org/10.1007/s10668-019-00583-2>
16. A. Shahzad, S. Hanif, Techno-economic feasibility of biogas generation in Attari village, Ferozepur road, Lahore. *Environ. Dev. Sustain.* **16**(5), 977–993 (2014). <https://doi.org/10.1007/s10668-013-9506-5>
17. N.R. Devela, B. Singh, T.C. Kandpal, Techno-economics of solar PV array-based hybrid systems for powering telecom towers. *Environ. Dev. Sustain.* **23**(11), 17003–17029 (2021). <https://doi.org/10.1007/s10668-021-01379-z>

18. A.S. Aziz, M.F.N. Tajuddin, M.R. Adzman, M.A.M. Ramli, Impacts of albedo and atmospheric conditions on the efficiency of solar energy: a case study in temperate climate of Choman, Iraq. *Environ. Dev. Sustain.* **23**(1), 989–1018 (2021). <https://doi.org/10.1007/s10668-019-00568-1>
19. T. Chen, M. Wang, R. Babaei, M.E. Safa, A.A. Shojaei, Technoeconomic analysis and optimization of hybrid solar-wind-hydrodiesel renewable energy systems using two dispatch strategies. *Int. J. Photoenergy* **2023** (2023). <https://doi.org/10.1155/2023/3101876>
20. A. Amirsolemani, R. Babaei, S.S. Mousavi Ajarostaghi, M. Saffari Pour, Feasibility evaluation of stand-alone energy solutions in energy-poor Islands using sustainable hydrogen production. *Int. J. Energy Res.* **46**(15), 24045–24063 (2022). <https://doi.org/10.1002/er.8704>
21. M.A. Mohamed, H.M. Abdullah, M.A. El-Meligy, M. Sharaf, A.T. Soliman, A. Hajjiah, A novel fuzzy cloud stochastic framework for energy management of renewable microgrids based on maximum deployment of electric vehicles. *Int. J. Electr. Power Energy Syst.* **129**, 106845 (2021). <https://doi.org/10.1016/j.ijepes.2021.106845>
22. M.A. Mohamed, T. Jin, W. Su, Multi-agent energy management of smart islands using primal-dual method of multipliers. *Energy* **208**, 118306 (2020). <https://doi.org/10.1016/j.energy.2020.118306>
23. H. Zou, J. Tao, S.K. Elsayed, E.E. Elattar, A. Almalaq, M.A. Mohamed, Stochastic multi-carrier energy management in the smart islands using reinforcement learning and unscented transform. *Int. J. Electr. Power Energy Syst.* **130**, 106988 (2021). <https://doi.org/10.1016/j.ijepes.2021.106988>
24. B. Bhandari, K.-T. Lee, C.S. Lee, C.-K. Song, R.K. Maskey, S.-H. Ahn, A novel off-grid hybrid power system comprised of solar photovoltaic, wind, and hydro energy sources. *Appl. Energy* **133**, 236–242 (2014). <https://doi.org/10.1016/j.apenergy.2014.07.033>
25. F.K. Abo-Elyousr, A. Elnozahy, Bi-objective economic feasibility of hybrid micro-grid systems with multiple fuel options for islanded areas in Egypt. *Renew. Energy* **128**, 37–56 (2018). <https://doi.org/10.1016/j.renene.2018.05.066>
26. M.K. Shahzad, A. Zahid, T. ur Rashid, M.A. Rehan, M. Ali, M. Ahmad, Techno-economic feasibility analysis of a solar-biomass off grid system for the electrification of remote rural areas in Pakistan using HOMER software. *Renew. Energy* **106**, 264–273 (2017). <https://doi.org/10.1016/j.renene.2017.01.033>
27. A. Oulis Rousis, D. Tzelepis, I. Konstantelos, C. Booth, G. Strbac, Design of a hybrid AC/DC microgrid using HOMER Pro: case study on an islanded residential application. *Inventions* **3**(3), 55 (2018). <https://doi.org/10.3390/inventions3030055>
28. M.H. Jahangir, S.A. Mousavi, R. Asayesh Zarchi, Implementing single- and multi-year sensitivity analyses to propose several feasible solutions for meeting the electricity demand in large-scale tourism sectors applying renewable systems. *Environ. Dev. Sustain.* **23**(10), 14494–14527 (2021). <https://doi.org/10.1007/s10668-021-01254-x>
29. H.Z. Al Garni, A. Awasthi, M.A.M. Ramli, Optimal design and analysis of grid-connected photovoltaic under different tracking systems using HOMER. *Energy Convers. Manag.* **155**, 42–57 (2018). <https://doi.org/10.1016/j.enconman.2017.10.090>
30. V. Boddapati, A.S.R. Nandikatti, S.A. Daniel, Techno-economic performance assessment and the effect of power evacuation curtailment of a 50 MWp grid-interactive solar power park. *Energy Sustain. Dev.* **62**, 16–28 (2021). <https://doi.org/10.1016/j.esd.2021.03.005>
31. R. Srivastava, A.N. Tiwari, V.K. Giri, An overview on performance of PV plants commissioned at different places in the world. *Energy Sustain. Dev.* **54**, 51–59 (2020). <https://doi.org/10.1016/j.esd.2019.10.004>
32. M.H.M. Sidek, N. Azis, W.Z.W. Hasan, M.Z.A. Ab Kadir, S. Shafie, M.A.M. Radzi, Automated positioning dual-axis solar tracking system with precision elevation and azimuth angle control. *Energy* **124**, 160–170 (2017). <https://doi.org/10.1016/j.energy.2017.02.001>
33. V. Sumathi, R. Jayapragash, A. Bakshi, P. Kumar Akella, Solar tracking methods to maximize PV system output—a review of the methods adopted in recent decade. *Renew. Sustain. Energy Rev.* **74**, 130–138 (2017). <https://doi.org/10.1016/j.rser.2017.02.013>
34. S. Sinha, S.S. Chandel, Analysis of fixed tilt and sun tracking photovoltaic–micro wind based hybrid power systems. *Energy Convers. Manag.* **115**, 265–275 (2016). <https://doi.org/10.1016/j.enconman.2016.02.056>

35. S. Bhakta, V. Mukherjee, Techno-economic viability analysis of fixed-tilt and two axis tracking stand-alone photovoltaic power system for Indian bio-climatic classification zones. *J. Renew. Sustain. Energy* **9**(1), 015902 (2017). <https://doi.org/10.1063/1.4976119>
36. C. Li, W. Yu, Techno-economic comparative analysis of off-grid hybrid photovoltaic/diesel/battery and photovoltaic/battery power systems for a household in Urumqi, China. *J. Clean. Prod.* **124**, 258–265 (2016). <https://doi.org/10.1016/j.jclepro.2016.03.002>
37. N.M. Kumar, J. Vishnupriyan, P. Sundaramoorthi, Techno-economic optimization and real-time comparison of sun tracking photovoltaic system for rural healthcare building. *J. Renew. Sustain. Energy* **11**(1), 015301 (2019). <https://doi.org/10.1063/1.5065366>
38. H. Al Garni, A. Awasthi, Techno-economic feasibility analysis of a solar PV grid-connected system with different tracking using HOMER software, in *2017 IEEE International Conference on Smart Energy Grid Engineering (SEGE)* (2017), pp. 217–222. <https://doi.org/10.1109/SEGE.2017.8052801>
39. S. Mubaarak et al., Techno-economic analysis of grid-connected PV and fuel cell hybrid system using different PV tracking techniques. *Appl. Sci.* **10**(23), 8515 (2020). <https://doi.org/10.3390/app10238515>
40. X. Liu et al., Techno-economic analysis of solar tracker-based hybrid energy systems in a rural residential building: a case study in South Africa. *Int. J. Green Energy* **00**(00), 1–20 (2022). <https://doi.org/10.1080/15435075.2021.2024545>
41. M.R. Elkadeem, S. Wang, S.W. Sharshir, E.G. Atia, Feasibility analysis and techno-economic design of grid-isolated hybrid renewable energy system for electrification of agriculture and irrigation area: a case study in Dongola, Sudan. *Energy Convers. Manag.* **196**, 1453–1478 (2019). <https://doi.org/10.1016/j.enconman.2019.06.085>
42. K. Kusakana, Techno-economic analysis of off-grid hydrokinetic-based hybrid energy systems for onshore/remote area in South Africa. *Energy* **68**, 947–957 (2014). <https://doi.org/10.1016/j.energy.2014.01.100>
43. Resources, NASA Prediction of Worldwide Energy Resources (2021). <https://power.larc.nasa.gov>
44. K. Kusakana, H.J. Vermaak, Hydrokinetic power generation for rural electricity supply: case of South Africa. *Renew. Energy* **55**, 467–473 (2013). <https://doi.org/10.1016/j.renene.2012.12.051>
45. R. Babaei, D.S.-K. Ting, R. Carriveau, Feasibility and optimal sizing analysis of stand-alone hybrid energy systems coupled with various battery technologies: a case study of Pelee Island. *Energy Rep.* **8**, 4747–4762 (2022). <https://doi.org/10.1016/j.egy.2022.03.133>
46. 1KW 2KW 3KW 5KW Windmill Generator System/2KW 3KW 5KW Wind Turbine Kit, “Alibaba.” [https://www.alibaba.com/product-detail/1KW-2KW-3KW-5KW-Windmill-Generator\\_60493711744.html?spm=a2700.details.0.0.5bce10144u6yxW](https://www.alibaba.com/product-detail/1KW-2KW-3KW-5KW-Windmill-Generator_60493711744.html?spm=a2700.details.0.0.5bce10144u6yxW)
47. ¢/KWH Levelized Cost of Electricity for Various Power and Energy Efficiency Options, National Hydropower Association. <https://www.hydro.org/waterpower/why-hydro/affordable>
48. C.S. Lai et al., Levelized cost of electricity for photovoltaic/biogas power plant hybrid system with electrical energy storage degradation costs. *Energy Convers. Manag.* **153**, 34–47 (2017). <https://doi.org/10.1016/j.enconman.2017.09.076>
49. M.R. Akhtari, M. Baneshi, Techno-economic assessment and optimization of a hybrid renewable co-supply of electricity, heat and hydrogen system to enhance performance by recovering excess electricity for a large energy consumer. *Energy Convers. Manag.* **188**, 131–141 (2019). <https://doi.org/10.1016/j.enconman.2019.03.067>
50. T. Salameh, M.A. Abdelkareem, A.G. Olabi, E.T. Sayed, M. Al-Chaderchi, H. Rezk, Integrated standalone hybrid solar PV, fuel cell and diesel generator power system for battery or supercapacitor storage systems in Khorfakkan, United Arab Emirates. *Int. J. Hydrogen Energy* **46**(8), 6014–6027 (2021). <https://doi.org/10.1016/j.ijhydene.2020.08.153>
51. M.H. Jahangir, S.A. Mousavi, M.A. Vaziri Rad, A techno-economic comparison of a photovoltaic/thermal organic Rankine cycle with several renewable hybrid systems for a residential area in Rayen, Iran. *Energy Convers. Manag.* **195**, 244–261 (2019). <https://doi.org/10.1016/j.enconman.2019.05.010>

52. T. Aderinto, H. Li, Ocean wave energy converters: status and challenges. *Energies* **11**(5), 1250 (2018). <https://doi.org/10.3390/en11051250>
53. M. Baneshi, F. Hadianfard, Techno-economic feasibility of hybrid diesel/PV/wind/battery electricity generation systems for non-residential large electricity consumers under southern Iran climate conditions. *Energy Convers. Manag.* **127**, 233–244 (2016). <https://doi.org/10.1016/j.enconman.2016.09.008>
54. S. Mandal, B.K. Das, N. Hoque, Optimum sizing of a stand-alone hybrid energy system for rural electrification in Bangladesh. *J. Clean. Prod.* **200**, 12–27 (2018). <https://doi.org/10.1016/j.jclepro.2018.07.257>
55. F. Fazelpour, N. Soltani, M.A. Rosen, Economic analysis of standalone hybrid energy systems for application in Tehran, Iran. *Int. J. Hydrogen Energy* **41**(19), 7732–7743 (2016). <https://doi.org/10.1016/j.ijhydene.2016.01.113>
56. C. Bordin, H.O. Anuta, A. Crossland, I.L. Gutierrez, C.J. Dent, D. Vigo, A linear programming approach for battery degradation analysis and optimization in offgrid power systems with solar energy integration. *Renew. Energy* **101**, 417–430 (2017). <https://doi.org/10.1016/j.renene.2016.08.066>
57. M.A. Vaziri Rad, A. Toopshekan, P. Rahdan, A. Kasaeian, O. Mahian, A comprehensive study of techno-economic and environmental features of different solar tracking systems for residential photovoltaic installations. *Renew. Sustain. Energy Rev.* **129**, 109923 (2020). <https://doi.org/10.1016/j.rser.2020.109923>
58. M. Shabani, J. Mahmoudimehr, Techno-economic role of PV tracking technology in a hybrid PV-hydroelectric standalone power system. *Appl. Energy* **212**, 84–108 (2018). <https://doi.org/10.1016/j.apenergy.2017.12.030>